IEEE Access
Multidisciplinary | Rapid Review | Open Access Journal

Received December 1, 2020, accepted December 16, 2020, date of publication December 30, 2020,
date of current version January 11, 2021.

Digital Object Identifier 10.1109/ACCESS.2020.3048147

Microwave Nondestructive Testing for Defect Detection in Composites Based on K-Means Clustering Algorithm

NAWAF H. M. M. SHRIFAN[1,2], GHASSAN NIHAD JAWAD[3], (Member, IEEE), NOR ASHIDI MAT ISA[1], AND MUHAMMAD FIRDAUS AKBAR[1], (Member, IEEE)

[1]School of Electrical and Electronic Engineering, Universiti Sains Malaysia, Pulau Pinang 14300, Malaysia
[2]Faculty of Oil and Minerals, University of Aden, Aden, Yemen
[3]Department of Electronics and Communications Engineering, University of Baghdad, Baghdad 10071, Iraq

Corresponding author: Muhammad Firdaus Akbar (firdaus.akbar@usm.my)

This work was supported by the Ministry of Education Malaysia Fundamental Research Grant Scheme (FRGS) under Grant 203.PELECT.6071430.

ABSTRACT Composite such as Glass Fibre Reinforced Polymer (GFRP) is increasingly used as insulation in many industrial applications such as the steel pipelines in the oil and gas industry. Due to ageing and cyclic operation, many hidden defects exist under insulation, such as corrosion and delamination. If these defects are not promptly detected and restored, the growth of defects causes a catastrophic loss. Therefore, an effective inspection technique using non-destructive testing (NDT) to detect the underneath defect is required. The ability of microwave signals to penetrate and interact with the inner structure within composites makes them a promising candidate for composite inspection. In the case of GFRP, the random patterns cause permittivity variations that influence the propagation of the microwave signals, which results in a blurred spatial image making the assessment of the material's state difficult. In this research, a novel microwave NDT technique is presented based on k-means unsupervised machine learning for defect detection in composites. At present, the defect evaluation using an unsupervised machine learning-based microwave NDT technique is not reported elsewhere. The unsupervised machine learning is employed to enhance the imaging efficiency and defect detection in GFRP. The technique is based on scanning the composite material with an open-ended rectangular waveguide operating from 18 to 26.5 GHz with 101 frequency points. The influence of the permittivity variations on the reflected coefficients due to the random patterns of GFRP is mitigated by measuring the mean of a set of the adjacent points at each operating frequency point using a small rectangular window. The measured data is converted to the time domain using a fast inverse Fourier transform (IFFT) to provide significant features and increase the signal resolution to 201-time steps. K-means algorithm is utilized to cluster the given features into the defect and defect-free regions in GFRP. The findings presented in this paper demonstrate the benefits of an unsupervised machine learning to detect a defect down to 1 mm, which is a considerable contribution over any existing defect inspection technique in composites.

INDEX TERMS Unsupervised machine learning, k-means, microwave NDT, defect detection.

I. INTRODUCTION

Early detection of defects under insulation is a critical problem in many industrial applications [1], including the pipeline in the oil and gas industry [2]. One of the main difficulties of tackling the problem relating to insulation is the inability to quickly detect and measure the severity of those areas that are suffering from various obscured defects such as corrosion, delamination, and cracks on the structure under insulation [3]. As these faults grow undetected, they can lead to critical system failures with many detrimental effects, including the risk to the safety of site workers [4], environmental disruption and economic effect on maintenance costs and production losses [5]. Therefore, a predictive inspection method evaluating the integrity of the structure is required to prevent these accidents using non-destructive testing (NDT) and to secure

The associate editor coordinating the review of this manuscript and approving it for publication was Wuliang Yin.

the safety and the health of the pipelines. Methods for evaluating pipeline damage are critical for saving maintenance costs, enhancing the integrity and reliability of the system [6].

Defect detection under insulation with conventional inspection methods such as eddy current and ultrasonic techniques are challenging due to the presence of the insulation layer that prevents direct access to the structure surface [7]. Ultrasonic methods applied to composites suffer from low signal to- noise ratio due to the anisotropic nature of the GFRP structure leads to reduce the probability of defect detection [8]. At the same time, inspection with eddy currents can be susceptible to magnetic permeability. Moreover, eddy currents technique is only applied to conductive materials [9], [10]. The current inspection routine to remove insulation material to facilitate inspection using a conventional technique such as ultrasonic, followed by re-application of insulation, is a costly and time-consuming process [11].

The microwave NDT system has therefore emerged as a promising solution to the identification and assessment of defects under insulation [6]. The microwave NDT method requires no physical contact with the surface or coupling and is capable of penetrating inside composite-based insulations. In comparison to ultrasonic and acoustic signals, microwave signals are capable of penetrating within dielectric insulations such as GFRP and interacting with their internal structure and are susceptible to changes related to boundary interfaces [12]. Electromagnetic waves penetrate a wide variety of non-conducting components at microwave frequencies, such as different composites, ceramics, concrete, and interfere with their internal structures. Microwave signals are non-ionizing and are not considered to induce dangerous radiation, resulting in a wide range of diverse imaging technologies becoming increasingly useful.

Several microwave NDT techniques have been reported for under insulation inspection, and the open-ended rectangular waveguide (OERW) inspection method is popular among them [13]–[17]. The working principle microwave NDT using OERWs is based on recording and analyzing the reflected, scattered electric field from an OERW probe scanned over a surface of the insulated structure using a calibrated Vector Network Analyzer (VNA). OERWs are widely used for microwave NDT applications such as dielectric property measurement of materials [13], the thickness measurement of dielectric slabs [14], [15], and porosity level estimation in ceramics [16]. Detecting the defects in under-insulated structures using open-ended rectangular waveguides also has been reported in [18]. However, an OERW approach has shown numerous limitations in detecting the delamination of non-homogeneous insulation, such as GRFP [19]. The spatial resolution of an OERW operating in the near field is a function of the probe dimensions. Hence, obtaining high-resolution images consist of accurate information of defect is very limited at microwave frequencies, especially when the probe dimensions are relatively larger than the dimension of defects. Besides, when concerned with randomly weaved pattern insulation such as GFRP, detecting the delamination under insulation is challenging at micrometer-range. Non-homogeneous properties of GFRP due to the random composition of fiberglass and epoxy resins render quantitative and selective frequency domain analysis ineffective to detect the delamination between a GFRP laminate and a steel pipe. The properties of the reflected microwave signals in the frequency domain can be substantially altered by these changes, which profoundly reduce the sensitivity of detecting any existing delamination.

Besides, other microwave NDT methods also reported in detecting the defects under GFRP insulation. In [20]–[22], a millimeter-wave active radiometer based on transmission measurement is used to detect and measure the delamination in GFRP. In the active thermographic method reported in [23], [24], the GFRP sample is illuminated with a waveguide and the differential temperature change is detected using a thermal camera. Furthermore, several microwave thermography techniques are recently reviewed for inspection of various composite structures in [25], [26]. Free space microwave NDT using horn lens antennas and a VNA is shown in [27], [28], while the use of interdigitated sensors to measure the S-parameters along a defected surface has been demonstrated in [29], [30]. Polarization studies on GFRP sample using the synthetic aperture radar technique are illustrated in [31], [32].

For identifying the defect source, various techniques are introduced. Time-domain reflectometry (TDR), as presented in [19] used inverse fast Fourier transform (IFFT) to identify two main peaks that refer to the sample surface and back metal. The back metal peak is recorded for defect representation. The reduction in the magnitude of the back metal peak is proportional to the defect presence. Similarly, terahertz time-domain spectroscopy (THz-TDS) is introduced in [33] for GFRP inspection. The technique aims to image the hidden objects that buried inside the GFRP layer in both transmission and reflection modes. The magnitude difference between the defected and non-defect regions is analyzed by monitoring the main peaks that refer to the sample layers such as front surface, buried object and rear surface. The difference in these peaks has been used for imaging the inspected sample which greatly improves defect detection. Moreover, principal component analysis (PCA) is employed for partitioning the acquired signal into three main sources in [34], [35]. The partitioned sources refer to the GFRP surface, the inner layer of GFRP and back metal. However, the information on the small defect may be covered by the components of the outer surface and inner layers of GFRP. Therefore, the features are not separated significantly which produce blurred edges of the defects. In addition, nonnegative matrix factorization (NMF) is introduced in [36], [37] to blindly separate the spatial frequency features into a defect and defect-free sources. However, NMF gives a different approximated result at each run time due to different initial optimization values. Moreover, NMF produces the worst result when there is a low spectral resolution [38]. The abovementioned techniques did not validate if the partitioned sources are already related

to the proposed sources theoretically. The first peak in TDR techniques, as well as the first component in PCA and NMF provides some information about the inner defect while they are proposed to handle the outer surface information, which is defect-free.

On the other hand, a microwave NDT is proposed in [39] based on machine learning techniques to provide a reliable inspection with a high accuracy rate of 99.62 %. Since the technique is limited to classifying the whole sample without defect assessment into defect and defect-free, the use of machine learning allows accurate identification of defects. In case of defect evaluation where the goal is classifying each inspected location into defect or defect-free, such as in [40], the classification is achieved using supervised-PCA features and support vector machine (SVM) classifier to locate the defected regions. The inspection is performed on a coated steel specimen to detect the corrosion undercoating. The last outcome value of the SVM classifier at each inspected location is used to construct a 2D binary image. Although several pixels were wrongly classified, the constructed image is displayed clearly in the corrosion places, which makes this technique capable of evaluating the corrosion location and size. However, the supervised machine learning techniques need training samples which difficult to be acquired in the practical application of NDT due to the variety of the samples' properties or the limited resources to acquire the training data.

Recent research has emerged to employ machine learning to measure the material's degradation [41]. The latest efforts to hybridise microwave NDT and machine learning inspecting complex systems (e.g. GFRP) have tremendous potential to increase the efficiency and reliability of inspection [6]. For example, the unsupervised k-means clustering algorithm as described in the next section is the most suitable technique to process the microwave signal in the time domain due to the simplicity of utilizing less training samples required by SVM and artificial neural network (ANN) techniques.

In this research, a novel microwave NDT technique is presented based on k-means unsupervised machine learning for defect detection in GFRP. At present, the defect evaluation using unsupervised machine learning-based microwave NDT technique is not reported elsewhere. The proposed technique is employed for defects detection and evaluation in terms of defect location and size. OERW is used to scan the GFRP sample by sweeping 101 frequency points from 18 to 26.5 GHz. The influence of the permittivity variations due to the random patterns of GFRP is mitigated by measuring the mean of a set of the adjacent points at each operating frequency point using a small rectangular window. IFFT is utilized to convert the signal from the frequency domain into the time domain as well as increase the resolution of the converted signal to 201-time steps. Simultaneously, the k-means algorithm is used to blindly classify the time domain data of each inspected location into separate clusters, such as defect and defect-free, to image the underneath defects. The work demonstrated in this manuscript is significant since the proposed technique capable of delivering an in-situ microwave NDT system for defect detection in complex composite material and may form part of quality control in manufacture as well as portable field service inspection.

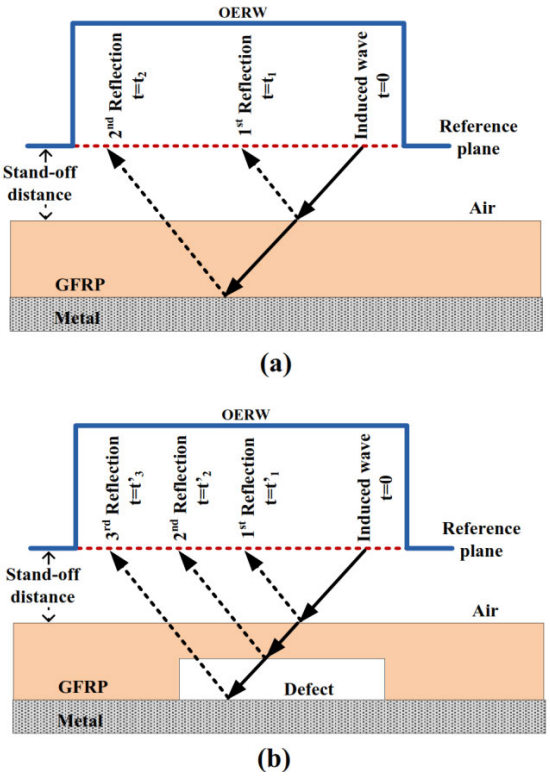

FIGURE 1. Cross-section diagram of the proposed scanning arrangement using an open-ended rectangular waveguide (not drawn to scale) in case of defect-free (a) and defect (b).

The findings presented in this research demonstrate the contribution of an unsupervised machine learning to detect a defect down to 1 mm, which is a considerable advantage over any existing defect inspection technique in composites. In this paper, a brief introduction to defect detection in the time domain and k-means clustering algorithm is introduced in section II. Section III explains the proposed microwave NDT technique. The result discussion is presented in sections IV. Finally, the conclusion is summarized in section V.

II. THEORETICAL BACKGROUND

A. MICROWAVE REFLECTION FOR DEFECT DETECTION

Figure 1 shows a cross-section of the microwave probe scanning arrangement in case of defect and defect-free. The reference plan of OERW is used to scan a metal-backed sample that consists of a dielectric layer which placed near the waveguide. Traditional TDR uses the time of receiving the reflection from a certain discontinuity to estimate the distance between it and the reference plane [17]. This implies knowledge of the speed at which the waves travel through the media under consideration, which is usually the speed of light. Therefore, two reflections can be obtained at different times in the case of defect-free, as shown in Figure 1(a).

The first reflection comes from the dielectric layer (e.g. GFRP), which arrives earlier at t_1. The second reflection is from the back metal surface, which comes late at t_2 due to the travelling distance between the waveguide and the back metal. In the case of defect presence, as shown in Figure 1(b), there are three reflections can be acquired which are from the dielectric surface, defect edge and the back metal at three different times, denoted as t_1', t_2' and t_3' respectively where $t_2' \neq t_2$. However, in the case of frequency sweeping, different frequency components travel at different velocities. Therefore, it is not possible to rely on the reflection time of arrival to determine the exact distance to the source of reflection. Moreover, the distance between the probe's end and the dielectric surface is assumed to be relatively small. This near-field condition implies that the dispersion effects such as pulse spreading and frequency chirping are reduced to a minimum.

Therefore, IFFT is usually used to obtain the discrete reflection coefficient in the time domain. Two main peaks can be identified at t_1 and t_2 in case of defect-free. In the other hand, two main peaks can be identified in case of defect presence which the first peak denotes to t_1' and the second peak denotes to a combination of t_2' and t_3' reflections. In the case of defect presence, the magnitude of the second peak t_2' is reduced compared to the second peak t_2 obtained from the defect-free sample. Therefore, any reduction in the magnitude of the second peak can provide information about the defect present in the dielectric layer. This observation can be employed to detect the defects under insulation in case of clustering two different sources, such as defect and defect-free signals.

B. K-MEANS CLUSTERING

The clustering process aims to group a given dataset of observations into separate clusters. The k-means clustering algorithm is one of the simplest unsupervised machine learning techniques to solve the clustering problem [42]. The procedure of k-means is to separate unlabeled dataset collection into a specific number of clusters (e.g. k groups). Each data point in the unlabeled dataset is assigned to one of the groups based on the similarity of the given features. Initially, the algorithm estimates the centroid of each group. The estimation can be done randomly by selecting a set of data points from the given dataset to represent each group centroid at the initial stage. Thereafter, the k-means algorithm works iteratively to reduce the clustering error by minimizing the objective function through achieving two main steps until reach the stopping criteria. Firstly, each data point in the dataset is assigned to the nearest cluster centroid, which the distance between them is the smallest compared to the other centroids. Secondly, the new centroid of each group is updated by calculating the mean of the data in each cluster. Finally, the algorithm stops the iteration when there is no change in the centroids' location or reach the maximum iterations number. Let, $X = \{x_1, x_2x_3 \ldots x_n\}$ is the unlabeled dataset to be clustered into k known groups and

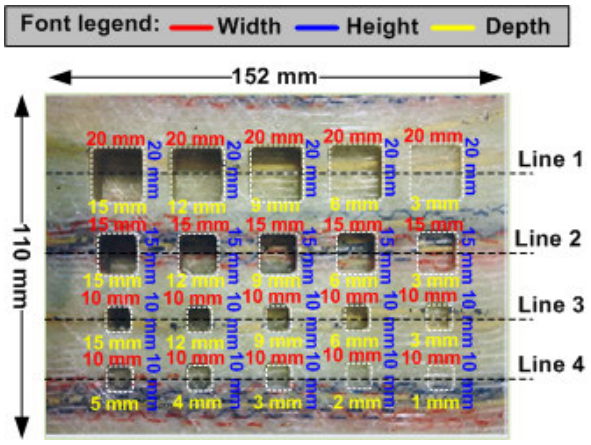

FIGURE 2. GFRP sample illustrates the defects' size and location.

$C = \{c_1, c_2c_3 \ldots c_m\}$ is the set of centroids where $m = k$ and $k \leq n$. The centroids are obtained by minimizing the objective function J as defined in equation (1).

$$J = \sum_{i=1}^{m} \sum_{j=1}^{n} ||X_j - C_i||^2 \tag{1}$$

where $||X_j - C_i||^2$ is the squared Euclidean distance between the data point X_j and the centroid C_i while n and m denote to the total number of the data points and number of cluster centroids respectively. Utilizing the Euclidean distance in this research provides a faster similarity metric with genuine appraisals compared to the other distance metrics [43]. The Euclidean distance is recommended as a distance measurement for time series data clustering as the nature of the utilized data in this research [44]. The update of the centroid C_i of each group is defined as in equation (2).

$$C_i = \frac{1}{N_{i,j}} \sum_{j=1}^{N_{i,j}} X_{i,j} \tag{2}$$

where $N_{i,j}$ refers to the number of the data points belong to i^{th} cluster centroid and $X_{i,j}$ denotes to the data points assigned to i^{th} cluster centroid. Thus, the k-means algorithm can be used to distinguish the different sources. In case of the defect and defect-free sources as explained in the next section, k-means can be employed for defect detection with microwave NDT.

III. THE PROPOSED METHOD

A. GFRP SAMPLE

Figure 2 illustrates the GFRP sample which composes the fibreglass and epoxy resins based matrix. This kind of composite is widely used in the oil and gas industry to reinforce the metal pipelines against the corrosion and high load of the pressure. The sample of thickness 23±0.32 mm includes various dimensions of defects such as air gaps are machinery etched in the sample layer. The size of the defects is ranged from 10 mm x 10 mm to 20 mm x 20 mm. On each horizontal line, the size of the defects is equally etched with a different degree of depth. The depth of the defects is back-drilled

TABLE 1. The dimension of the GFRP sample.

Parameter	Value
Sample size	152 mm x 110 mm
Sample thickness	23±0.32 mm
Defect dimension	10 mm x 10 mm, 15 mm x 15 mm, and 20 mm x 20 mm
Defect depth	a) 3 mm to 15 mm with a step size of 3 mm b) 1 mm to 5 mm with a step size of 1 mm

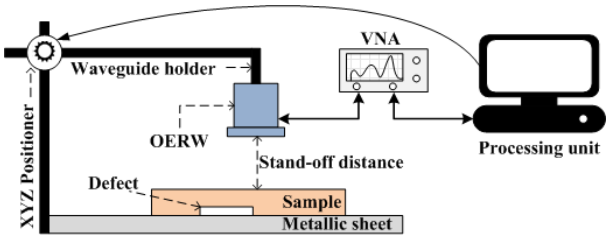

FIGURE 3. The setup diagram of the microwave NDT system.

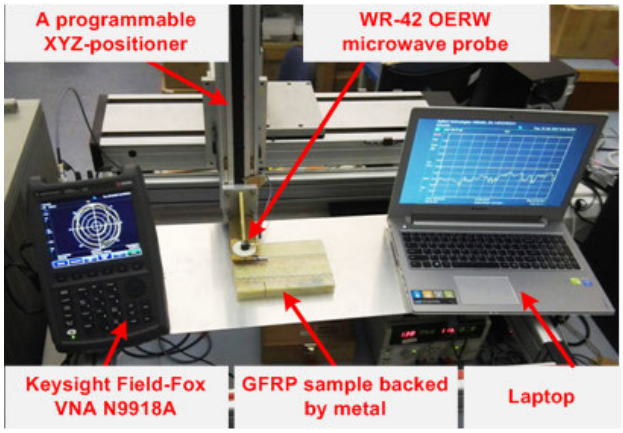

FIGURE 4. Illustration of the utilized instruments for defect detection in GFRP sample.

and ranging from 1mm to 15 mm. The dimensions of the GFRP sample are detailed in Table 1. Additionally, Figure 2 illustrates the dimensions of every single defect independently. The face of the defects is placed on the metal during the inspection to simulate the underneath defects between the GFRP layer and metal, whilst leaving its top surface undisturbed.

B. INSPECTION TECHNIQUE

Figure 3 shows the experimental setup diagram of the inspection technique. The standard WR-42 OERW microwave probe with an aperture size of 10.6 x 4.3 mm^2 raster-scanned with a step size of 2 mm in the x- and y-directions is shown in Figure 4. The scanning is achieved on 80 and 54 points in x- and y-directions, respectively. The standoff distance

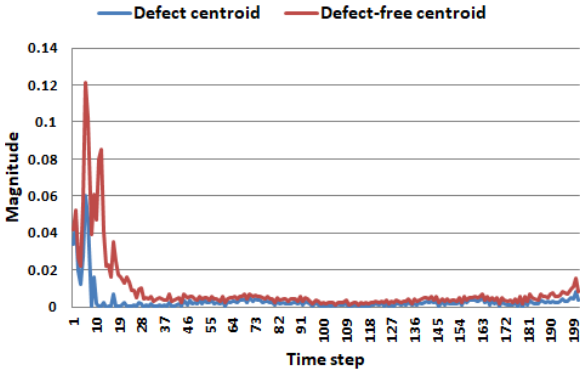

FIGURE 5. The initial centroids of the defect and defect-free sources.

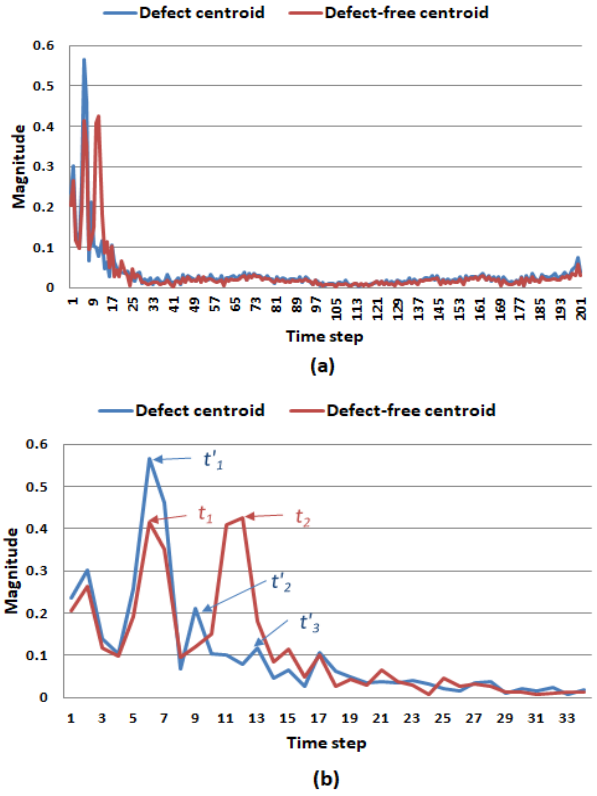

FIGURE 6. The optimal centroids of the defect and defect-free sources converged by the k-means algorithm (a), the peaks' distribution of the defect and defect-free for the first 35 time steps (b).

between the OERW probe and the sample is set to 1 mm. The programmable positioner is used to control the waveguide movement during the inspection process. One port calibration is carried out to effectively shift the measurement reference plane to the end of the microwave cable (input port of waveguide). Upon successful calibration, the systematic errors of Vector Network Analyzer (VNA), the connectors and cables used to connect the VNA to the waveguide are eliminated from measurements. A portable Keysight Field-Fox VNA (N9918A) is used to measure the complex reflection coefficients from 18 to 26.5 GHz, as a linear sweep with 101 frequency points at each inspected location. As a result of the inspection, a 3D matrix $d(x, y, f)$ is constructed where x

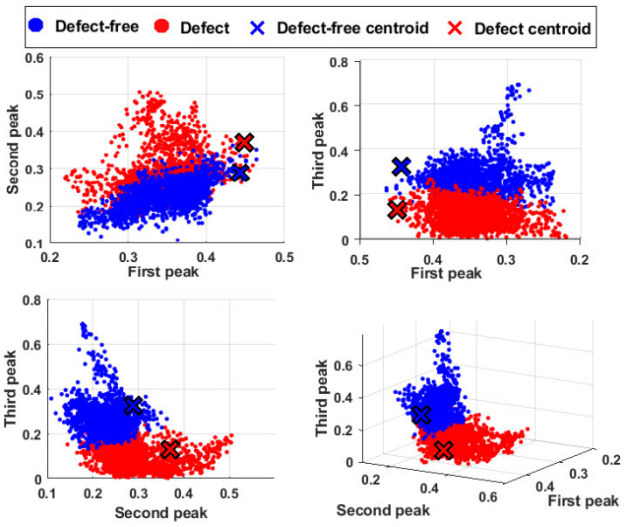

FIGURE 7. Scattering plots illustrate the data points at the location of the main three peaks t_2', t_2' and t_3' with respect to the defect and defect-free clusters for each inspected location.

and y denote to the inspected location and f denotes to the operational frequency point from 1 to 101.

C. MICROWAVE SIGNAL PROCESSING

Although the acquired data $d(x, y, f)$ at each frequency point can image the inspected sample. However, the generated images cannot provide information about all the defects of the GFRP sample. In the case of GFRP inspection, the randomly weaved patterns cause permittivity variations that influence the properties of the reflected microwave signals. Therefore, the uniformity of the defects shapes should be maintained to simplify the assessment of the defect's size and location. In this section, a rectangular window with size $a \times b$ is proposed which is near to the half of the probe aperture dimensions as the inspection step achieved by 2mm in x and y-directions where $a = 3$ and $b = 4$. Therefore, the values of a and b have been chosen as a trade-off between fixing the spatial abnormality in the woven medium and the ability of the technique to provide an accurate location for small defects. The window is moved on each frequency image to crop the corresponding frequency coefficients. Thereafter, the mean of the cropped coefficients is measured to mitigate the effects of the random patterns of the GFRP sample. The outcome of this process generates a 3D matrix named D with dimensions $X - a$ and $Y - b$ for each frequency point f. Equation (3) formulates the window sliding on the acquired microwave data d.

$$D(x, y, f) = \frac{1}{a \times b} \sum_{n=x, m=y}^{N, M} d(n, m, f) \tag{3}$$

where the boundary of N and M is described as the following equations at each x and y step.

$$N = x + a - 1 \tag{4}$$

$$M = y + b - 1 \tag{5}$$

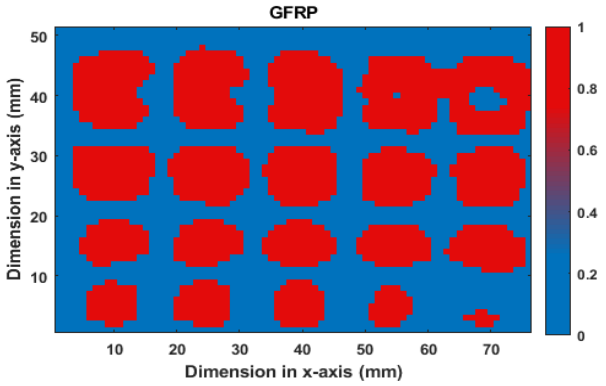

FIGURE 8. The clustering result of GFRP sample using the proposed technique.

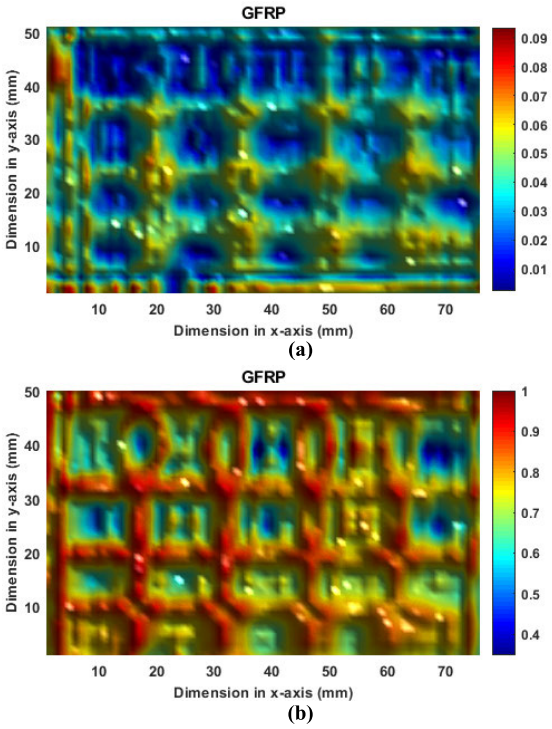

FIGURE 9. The imaging results of GFRP using TDR in [19] (a), and correlation technique in [18].

The IFFT is used to obtain the discrete reflection coefficient in the time domain. Therefore, the 101 frequency points at each $D(x, y)$ are converted from the frequency domain into the time domain using IFFT. The resolution of the 101 frequency points is extended to 201-time steps using IFFT function in Matlab (R2019a) to ensure the magnitude each peak in the time domain reaches its maximum value. The converted data is reshaped into T matrix with rows number $(X - a) \times (Y - b)$ and 201 columns to be clustered blindly into the defect and defect-free using the k-means algorithm.

D. DEFECT DETECTION

The magnitude of the time-domain data T which obtained using IFFT is clustered into two groups using the k-means algorithm to distinguish between the defect and defect-free

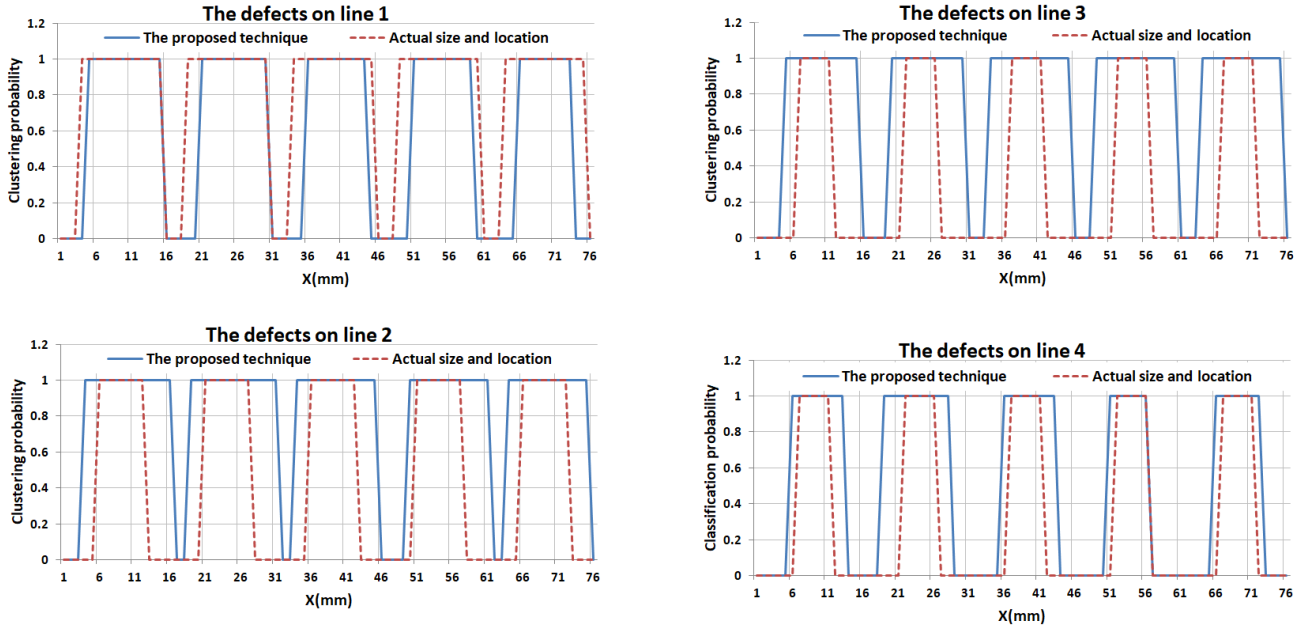

FIGURE 10. A comparison between the result of the proposed technique with the actual defects' size and location of the GFRP sample.

regions. Figure 5 shows the initial two centroids of the k-means algorithm. The centroids' boundaries are established based on the magnitude of the defect-free source is greater than the magnitude of the defective source due to the peaks' reduction in case of defect presence as explained in section 2(A). Moreover, the constructed centroids in a guided way aim to avoid establishing the centroids randomly which may lead to different clustering results as well as reducing the processing time. The initial centroids of the defect and defect-free are constructed as in equations (6) and (7).

$$c^{f}_{1,n} = \max(T_n) \tag{6}$$

$$c^{d}_{2,n} = \min(T_n) \tag{7}$$

where $c^{f}_{1,n}$ and $c^{d}_{2,n}$ denote to the initial centroids of the defect-free and defect respectively while n denotes to the number of time steps.

IV. RESULTS AND DISCUSSION

Figure 6(a) shows the optimal centroids of the defect and defect-free sources obtained by the k-means algorithm. A number of 12 iterations were performed by the k-means until converging the final outcome of the optimal centroids. This number of iterations refers to the number of the centroids' modifications due to the mean measurement of each cluster. At the final iteration, there is no centroids' changes have occurred. Therefore, the k-means reaches the stop criteria and the clustering results are converged. Figure 6(b) zooms in the peaks' distribution of the first 35 time steps of the converged centroids. It can be noted that the k-means algorithm is capable of distinguishing between the sources of the defect and defect-free based on the assumed approach in section 2(A). The peaks' distribution in the defect-free centroid shows the first peak t_1 and the second peak t_2 which are obtained from the GFRP surface and the back metal, respectively. On the other hand, the peaks' distribution in the defective centroid shows three peaks t'_1, t'_2 and t'_3 which are obtained from the surface of the GFRP sample, defect edge and the back metal respectively. Therefore, the k-means partitioned the microwave reflected coefficients of the defect and defect-free regions based on the similarity to those centroids. Thus, the capability of the k-means algorithm to distinguish between the defect and defect-free sources based on microwave signals is validated.

Figure 7 shows an example of the scattered data points from different 3D projections. The data points are obtained from the first, second and third peaks at 6, 9, 13-time steps respectively. At these time steps, the data points are obtained from each scanned location. The centroid of each cluster is placed nearby its data points at the final stage of the clustering process. The data point is classified to its closest centroid based on the Euclidean distance. The data point has a minimum Euclidean distance to the defect-free centroid is classified as a defect-free location. Similarly, the data point has a minimum Euclidean distance to the defect centroid is classified as a defected location. Thus, the clustering of GFRP sample has been done into defect and defect-free locations.

Figure 8 illustrates the clustering results in which all the defects in the GFRP sample are detected using the proposed technique. The proposed technique is capable to effectively detect the small size defect with 1mm depth on line 4 compared to the imaging result of [19] and [18] as shown in Figure 9 (a) and (b), respectively. Moreover, the proposed technique is capable to sharply separate the edges

of the large size defects on the first line compared to the merged defects result by the compared techniques. The large size defects in [19] and [18] are illustrated as one contentious defect, which makes the defect assessment difficult. The proposed technique sharps the edges of the large size defects, which facilitates the defect evaluation.

Figure 10 illustrates a comparison between the clustering results to the actual location and size of the GFRP sample. All the defects are distributed corresponding to the actual location. Although the significant results of the detection, the size of the defects seems larger than the actual size, especially the defects on lines 2 to 4. The large size of the defects belongs to the large size of the waveguide aperture which is 10.6×4.3 mm^2. During the scanning process, a part of the waveguide aperture enters the defected area, which makes a reduction in the microwave signal even the rest of the aperture remains in the sound region. The occurred reduction is correlated to the defect's source during the clustering process which leads to large defects' size. Furthermore, supervised machine learning such as ANN and SVM may provide significant results in term of the defect's size due to the learning-based process while a suitable training sample is provided. Therefore, a small size aperture will be evaluated using the proposed technique besides various supervised machine learning algorithms in future work.

V. CONCLUSION

The work demonstrated in this manuscript presents a novel microwave NDT technique based on k-means unsupervised machine learning for defect detection in GFRP. At present, the defect evaluation in terms of defect location and size using an unsupervised machine learning-based microwave NDT technique is not reported elsewhere. The proposed technique is employed to detect underneath defects in the GFRP layer based on microwave reflection coefficients. The influence of the permittivity variations on the reflected coefficients due to the random patterns of GFRP is mitigated by measuring the mean of a set of the adjacent points at each frequency point using a small rectangular window. Thereafter, the frequency coefficients are converted into the time domain using IFFT. The resolution of the acquired 101 frequency points is extended into 201-time steps for allowing each peak in the time domain to reach its maximum value. Finally, the time domain data of each location is blindly clustered using the k-mean algorithm into defect or defect-free to detect and image the underneath defects in the GFRP layer.

Nevertheless, the size of the defect seems larger than the actual size; the proposed method significantly detected the small size defect down to 1mm depth of defect compared to other methods presented in the literature. The proposed method is capable to sharply separate the edges of the defects and the defect-free regions among the defects are clearly illustrated. The simplicity of the proposed technique due to fewer customizations makes it operational friendly and can be used as an in-situ microwave NDT system of detecting and imaging the defect and may form part of quality control in manufacture as well as portable field service inspection.

REFERENCES

[1] H. Deng, Z. He, and L. Chen, "Ultrasonic guided wave-based detection of composite insulator debonding," *IEEE Trans. Dielectr. Electr. Insul.*, vol. 24, no. 6, pp. 3586–3593, Dec. 2017.

[2] M. S. Ur Rahman, A. Haryono, and M. A. Abou-Khousa, "Microwave non-destructive evaluation of glass reinforced epoxy and high density polyethylene pipes," *J. Nondestruct. Eval.*, vol. 39, no. 1, p. 26, Mar. 2020.

[3] E. O. Eltai, F. Musharavati, and E.-S. Mahdi, "Severity of corrosion under insulation (CUI) to structures and strategies to detect it," *Corrosion Rev.*, vol. 37, no. 6, pp. 553–564, Nov. 2019.

[4] A. V. Yavorskyi, M. O. Karpash, L. Y. Zhovtulia, L. Y. Poberezhny, and P. O. Maruschak, "Safe operation of engineering structures in the oil and gas industry," *J. Natural Gas Sci. Eng.*, vol. 46, pp. 289–295, Oct. 2017.

[5] A. Ghavamian, F. Mustapha, B. T. Baharudin, and N. Yidris, "Detection, localisation and assessment of defects in pipes using guided wave techniques: A review," *Sensors*, vol. 18, no. 12, p. 4470, Dec. 2018.

[6] N. H. M. M. Shrifan, M. F. Akbar, and N. A. M. Isa, "Prospect of using artificial intelligence for microwave nondestructive testing technique: A review," *IEEE Access*, vol. 7, pp. 110628–110650, 2019.

[7] C. Xu, W. Zhang, C. Wu, J. Xie, X. Yin, and G. Chen, "An improved method of eddy current pulsed thermography to detect subsurface defects in glass fiber reinforced polymer composites," *Compos. Struct.*, vol. 242, Jun. 2020, Art. no. 112145.

[8] H. Taheri and A. A. Hassen, "Nondestructive ultrasonic inspection of composite materials: A comparative advantage of phased array ultrasonic," *Appl. Sci.*, vol. 9, no. 8, p. 1628, Apr. 2019.

[9] Y. Deng and X. Liu, "Electromagnetic imaging methods for nondestructive evaluation applications," *Sensors*, vol. 11, no. 12, pp. 11774–11808, Dec. 2011.

[10] J. García-Martín, J. Gómez-Gil, and E. Vázquez-Sánchez, "Non-destructive techniques based on eddy current testing," *Sensors*, vol. 11, no. 3, pp. 2525–2565, Feb. 2011.

[11] M. F. Akbar, R. Sloan, C. I. Duff, M. Wielgat, and J. F. Knowles, "Nondestructive testing of thermal barrier coated turbine blades using microwave techniques," *Mater. Eval.*, vol. 74, no. 4, pp. 543–551, 2016.

[12] Z. Li, P. Wang, A. Haigh, C. Soutis, and A. Gibson, "Review of microwave techniques used in the manufacture and fault detection of aircraft composites," *Aeronaut. J.*, vol. 125, no. 1283, pp. 151–179, Jan. 2021.

[13] Z. Li, A. Haigh, C. Soutis, A. Gibson, and R. Sloan, "A simulation-assisted non-destructive approach for permittivity measurement using an open-ended microwave waveguide," *J. Nondestruct. Eval.*, vol. 37, no. 3, p. 39, Sep. 2018.

[14] M. T. Ghasr, M. J. Horst, M. Lechuga, R. Rapoza, C. J. Renoud, and R. Zoughi, "Accurate one-sided microwave thickness evaluation of lined-fiberglass composites," *IEEE Trans. Instrum. Meas.*, vol. 64, no. 10, pp. 2802–2812, Oct. 2015.

[15] R. Zoughi, J. R. Gallion, and M. T. Ghasr, "Accurate microwave measurement of coating thickness on carbon composite substrates," *IEEE Trans. Instrum. Meas.*, vol. 65, no. 4, pp. 951–953, Apr. 2016.

[16] M. F. Akbar, G. N. Jawad, C. I. Duff, and R. Sloan, "Porosity evaluation of in-service thermal barrier coated turbine blades using a microwave nondestructive technique," *NDT E Int.*, vol. 93, pp. 64–77, Jan. 2018.

[17] M. F. Akbar, G. N. Jawad, L. D. Rashid, and R. Sloan, "Nondestructive evaluation of coatings delamination using microwave time domain reflectometry technique," *IEEE Access*, vol. 8, pp. 114833–114841, 2020.

[18] A. J. K. M. Firdaus, R. Sloan, C. I. Duff, M. Wielgat, and J. F. Knowles, "Microwave nondestructive evaluation of thermal barrier coated turbine blades using correlation analysis," in *Proc. 46th Eur. Microw. Conf. (EuMC)*, Oct. 2016, pp. 520–523.

[19] M. F. Akbar, G. N. Jawad, L. R. Danoon, and R. Sloan, "Delamination detection in glass-fibre reinforced polymer (GFRP) using microwave time domain reflectometry," in *Proc. 15th Eur. Radar Conf. (EuRAD)*, Sep. 2018, pp. 253–256.

[20] C. Viegas, B. Alderman, P. G. Huggard, J. Powell, K. Parow-Souchon, M. Firdaus, H. Liu, C. I. Duff, and R. Sloan, "Active millimeter-wave radiometry for nondestructive testing/evaluation of composites—Glass fiber reinforced polymer," *IEEE Trans. Microw. Theory Techn.*, vol. 65, no. 2, pp. 641–650, Feb. 2017.

[21] D. K. Hsu, K.-S. Lee, J.-W. Park, Y.-D. Woo, and K.-H. Im, "NDE inspection of terahertz waves in wind turbine composites," *Int. J. Precis. Eng. Manuf.*, vol. 13, no. 7, pp. 1183–1189, Jul. 2012.
[22] Z. Li, A. Haigh, C. Soutis, A. Gibson, and R. Sloan, "Microwaves sensor for wind turbine blade inspection," *Appl. Compos. Mater.*, vol. 24, no. 2, pp. 495–512, Apr. 2017.
[23] A. Mirala, A. Foudazi, M. T. A. Qaseer, and K. M. Donnell, "Active microwave thermography to detect and locate water ingress," *IEEE Trans. Instrum. Meas.*, vol. 69, no. 12, pp. 9774–9783, Dec. 2020.
[24] R. Meredith, *Engineers' Handbook of Industrial Microwave Heating*. Stevenage, U.K.: Institution Engineering Technology, 1998.
[25] F. Ciampa, P. Mahmoodi, F. Pinto, and M. Meo, "Recent advances in active infrared thermography for non-destructive testing of aerospace components," *Sensors*, vol. 18, no. 2, p. 609, Feb. 2018.
[26] H. Zhang, R. Yang, Y. He, A. Foudazi, L. Cheng, and G. Tian, "A review of microwave thermography nondestructive testing and evaluation," *Sensors*, vol. 17, no. 5, p. 1123, May 2017.
[27] N. Hamzah, D. K. Ghodgaonkar, K. F. Che Kasim, and Z. Awang, "Microwave non-destructive testing of coatings and paints using free space microwave measurement," *Sci. Res. J.*, vol. 2, no. 2, p. 17, Dec. 2005.
[28] I. Zivkovic and A. Murk, "Free-space transmission method for the characterization of dielectric and magnetic materials at microwave frequencies," in *Microwave Materials Characterization*, S. Costanzo, Ed. Rijeka, Croatia: InTech, 2012, pp. 73–90, doi: 10.5772/51596.
[29] B. M. Abdullah, J. Cullen, A. Mason, and A. I. Al-Shamma'a, "A novel method for monitoring structural metallic materials using microwave NDT," in *Sensing Technology: Current Status and Future Trends I* (Smart Sensors, Measurement and Instrumentation). Cham, Switzerland: Springer, 2014, pp. 161–180, doi: 10.1007/978-3-319-02318-2_9.
[30] L. Li, X. Yang, Y. Yin, J. Yuan, X. Li, L. Li, and K. Huang, "An interdigital electrode probe for detection, localization and evaluation of surface notch-type damage in metals," *Sensors*, vol. 18, no. 2, p. 371, Jan. 2018.
[31] O. Büyüköztürk and T.-Y. Yu, "Far-field radar NDT technique for detecting GFRP debonding from concrete," *Construct. Building Mater.*, vol. 23, no. 4, pp. 1678–1689, Apr. 2009.
[32] T.-Y. Yu and O. Büyüköztürk, "A far-field airborne radar NDT technique for detecting debonding in GFRP–retrofitted concrete structures," *NDT E Int.*, vol. 41, no. 1, pp. 10–24, Jan. 2008.
[33] J. Wang, J. Zhang, T. Chang, L. Liu, and H.-L. Cui, "Terahertz nondestructive imaging for foreign object detection in glass fibre-reinforced polymer composite panels," *Infr. Phys. Technol.*, vol. 98, pp. 36–44, May 2019.
[34] H. Zhang, B. Gao, G. Y. Tian, W. L. Woo, and L. Bai, "Metal defects sizing and detection under thick coating using microwave NDT," *NDT E Int.*, vol. 60, pp. 52–61, Dec. 2013.
[35] H. Zhang, L. Xu, R. Wu, and A. Simm, "Sweep frequency microwave NDT for subsurface defect detection in GFRP," *Insight—Non-Destructive Test. Condition Monitor.*, vol. 60, no. 3, pp. 123–129, Mar. 2018.
[36] B. Gao, H. Zhang, W. L. Woo, G. Y. Tian, L. Bai, and A. Yin, "Smooth nonnegative matrix factorization for defect detection using microwave nondestructive testing and evaluation," *IEEE Trans. Instrum. Meas.*, vol. 63, no. 4, pp. 923–934, Apr. 2014.
[37] H. Zhang, B. Gao, G. Yun Tian, W. Lok Woo, and A. Simm, "Spatial-frequency spectrum characteristics analysis with different lift-offs for microwave nondestructive testing and evaluation using Itakura-Saito nonnegative matrix factorization," *IEEE Sensors J.*, vol. 14, no. 6, pp. 1822–1830, Jun. 2014.
[38] B. Qin, C. Hu, and S. Huang, "Target/background classification regularized nonnegative matrix factorization for fluorescence unmixing," *IEEE Trans. Instrum. Meas.*, vol. 65, no. 4, pp. 874–889, Apr. 2016.
[39] A. Ali, B. Hu, and O. Ramahi, "Intelligent detection of cracks in metallic surfaces using a waveguide sensor loaded with metamaterial elements," *Sensors*, vol. 15, no. 5, pp. 11402–11416, May 2015.
[40] A. Ali, A. Albasir, and O. M. Ramahi, "Microwave sensor for imaging corrosion under coatings utilizing pattern recognition," in *Proc. IEEE Int. Symp. Antennas Propag. (APSURSI)*, Jun. 2016, pp. 951–952.
[41] L. Yin, B. Ye, Z. Zhang, Y. Tao, H. Xu, J. R. S. Avila, and W. Yin, "A novel feature extraction method of eddy current testing for defect detection based on machine learning," *NDT E Int.*, vol. 107, Oct. 2019, Art. no. 102108.
[42] T. Kanungo, D. M. Mount, N. S. Netanyahu, C. D. Piatko, R. Silverman, and A. Y. Wu, "An efficient K-means clustering algorithm: Analysis and implementation," *IEEE Trans. Pattern Anal. Mach. Intell.*, vol. 24, no. 7, pp. 881–892, Jul. 2002.
[43] M. S. Ahuja and L. Singh, "A novel approach of detecting frauds in ecommerce sites by hybridizing KNN and Euclidean distance mechanism," *Int. J. Adv. Res. Comput. Sci.*, vol. 8, no. 5, pp. 2169–2172, 2017.
[44] M. R. Berthold and F. Höppner, "On clustering time series using Euclidean distance and pearson correlation," 2016, *arXiv:1601.02213*. [Online]. Available: http://arxiv.org/abs/1601.02213

NAWAF H. M. M. SHRIFAN received the bachelor's degree in computer science and engineering from the University of Aden, Aden, Yemen, in 2006, and the M.Sc. degree in informatics from Universiti Sains Malaysia (USM), Pulau Pinang, Malaysia, in 2017, where he is currently pursuing the Ph.D. degree in microwave nondestructive testing with the School of Electrical and Electronic Engineering. Since 2008, he has been a permanent Lecturer with the Department of Oil and Gas Engineering, Faculty of Oil and Minerals, University of Aden.

GHASSAN NIHAD JAWAD (Member, IEEE) was born in Baghdad, Iraq, in 1984. He received the B.Sc. and M.Sc. degrees in electronics and communication engineering from the University of Baghdad, Baghdad, in 2005 and 2009, respectively, and the Ph.D. degree from The University of Manchester, in 2016. From 2006 to 2009, he was with Orascom Telecom Iraq (Zain Iraq later), as a Network Switching Engineer. He is currently a Lecturer with the University of Baghdad. His current research interests include microwave and millimetre-wave passive components, gyrotropic microwave devices, microwave non-destructive testing techniques, and short-range radar systems.

NOR ASHIDI MAT ISA received the B.Eng. degree (Hons.) in electrical and electronic engineering from Universiti Sains Malaysia (USM), in 1999, and the Ph.D. degree in electronic engineering (majoring in image processing and artificial neural network), in 2003. He is currently a Professor and the Deputy Dean (Academic, Career, and International) with the School of Electrical and Electronic Engineering, USM. His research interests include intelligent systems, image processing, neural network, biomedical engineering, and intelligent diagnostic systems and algorithms.

MUHAMMAD FIRDAUS AKBAR (Member, IEEE) received the B.Sc. degree in communication engineering from International Islamic University Malaysia (IIUM), Malaysia, in 2010, and the M.Sc. and Ph.D. degrees from The University of Manchester, Manchester, U.K., in 2012 and 2018, respectively. From 2010 to 2011, he was with Motorola Solutions, Penang, Malaysia, as a Research and Development Engineer. From 2012 to 2014, he was an Electrical Engineer with Usains Infotech Sdn Bhd, Penang. He is currently a Senior Lecturer at Universiti Sains Malaysia (USM). He is also the Founder and the Director of Visionlytics Sdn Bhd. His current research interests include electromagnetics, microwave non-destructive testing, and microwave sensor and imaging.